Received 15 April 2018
Revised 19 August 2018
Accepted 2 September 2018

Direct torque control of dual star induction motor using a fuzzy-PSO hybrid approach

Ghoulemallah Boukhalfa, Sebti Belkacem, Abdesselem Chikhi and Said Benaggoune
Department of Electrical Engineering, Faculty of Technology, University of Batna2, Fesdis, Algeria

Abstract
This paper presents the particle swarm optimization (PSO) algorithm in conjuction with the fuzzy logic method in order to achieve an optimized tuning of a proportional integral derivative controller (PID) in the DTC control loops of dual star induction motor (DSIM). The fuzzy controller is insensitive to parametric variations, however, with the PSO-based optimization approach we obtain a judicious choice of the gains to make the system more robust. According to Matlab simulation, the results demonstrate that the hybrid DTC of DSIM improves the speed loop response, ensures the system stability, reduces the steady state error and enhances the rising time. Moreover, with this controller, the disturbances do not affect the motor performances.

Keywords Dual stator induction motor (DSIM), Direct torque control (DTC), Speed control, particle swarm optimization (PSO), Fuzzy logic control (FLC)
Paper type Review Article

Nomenclature

P	Number of pole pairs	$\mathrm{R_r}$	Rotor resistance
J	The moment of inertia	$\mathrm{L_{s1}}$, $\mathrm{L_{s2}}$	Stators inductances
f_r	The friction coefficient	$\mathrm{L_r}$	Rotor Inductance
T_{em}	The electromagnetic torque	$\mathrm{L_m}$	Mutual inductance
		n	number of particles in the group
T_{r}	The load torque		
Ω_{r}	is the mechanical rotation speed of the rotor	d	dimension index
		t	pointer of iterations (generations)
$\mathrm{R_{s1}}$, $\mathrm{R_{s2}}$	Stators resistances		

Publishers note: The publisher wishes to inform readers that the article "Direct torque control of dual star induction motor using a fuzzy-PSO hybrid approach" was originally published by the previous publisher of *Applied Computing and Informatics* and the pagination of this article has been subsequently changed. There has been no change to the content of the article. This change was necessary for the journal to transition from the previous publisher to the new one. The publisher sincerely apologises for any inconvenience caused. To access and cite this article, please use Boukhalfa, G., Belkacem, S., Chikhi, A., Benaggoune, S. (2022), "Direct torque control of dual star induction motor using a fuzzy-PSO hybrid approach", *Applied Computing and Informatics*. Vol. 18 No. 1/2, pp. 74-89. The original publication date for this paper was 06/09/2018.

$v^t_{i,m}$	velocity of particle at iteration I		stators and rotor, respectively
w	inertia weight factor	subscripts *1, 2*	denote variables and parameters of stator *1* and *2* respectively
rand ()	random number between *0* and *1*		
$pbest_i$	best previous position of the *ith* particle	V_{ds1}, V_{qs1}, V_{ds2}, V_{qs2}	respectively stator voltages in the *d-q* axis
gbest	best particle among all the particles in the population	I_{ds1}, I_{qs1}, I_{ds2}, I_{qs2}	components of the stator currents in the d - q axis
		I_{dr}, I_{qr}	the rotor currents
C_1,C_2	acceleration constant	ψ_{ds1}, ψ_{qs1}, ψ_{ds2}, ψ_{qs2}	components of the stator flux linkage vectors in *d-q* axis
subscripts *s*, *r*	indicate the variables and parameters of		
		ψ_{dr}, ψ_{qr}	respectively rotor fluxes

1. Introduction

In high-power applications, the dual star induction motor has largely replaced the induction machines whose roles were predominant in the industry [1–5]. The dual star induction motor is constituted of two windings with phases shifted from one another by an angle of 30 electrical degrees. These windings are usually powered by a six-phase inverter fed by variable speed drives. The main advantages of the DSIM are: [6] their higher torque density, reduced harmonic content of the DC link current and the reliability of this machine which allows a functioning with one or several phases of defective motor. However the control of DSIM is considered to be complicated because the difficulty of obtaining the decoupling of the torque and the flux. To overcome these difficulties, high-performance algorithms have been developed [7–14].

To satisfy the performance of an electromechanical system drive, the generally used strategy consists in controlling the speed by a PID controller to cancel the static error and reduce the response time. This speed is often characterized by an overshoot at startup and depends on the parameters of the machine. In order to overcome these complications, several methods have been developed to adjust the PID regulator.

Auto-tuning is one of these methods, which is used in PID controllers [15]. The performance of the control loops is improved by automatically adjusting the PID gain parameters of the conventional controllers.

The self-tuning method has been suggested by many researchers [16,17]. A self-adjusting mechanism has been set up to adapt the PID regulator in case of any disturbances.

The use of optimization algorithms as alternative methods for tuning PID controllers has been a recent topic of research in electric machines control. New optimization techniques are proposed, for instance, the Imperialist Competitive Algorithm (ICA) [18], evolutionary algorithm [19], Genetic Algorithm (GA) [20–21], BAT algorithm [22] ,Particle Swarm Optimization (PSO) [23–26], and Ant Colony Optimization (ACO) algorithm [27], Harmony Search (HS) [28], hybrid GA [29–30], adaptive Cuckoo Search algorithm (CS) [31].

PSO was first used by Eberhart and Kennedy in 1995 [32]. This approach is inspired by the social behavior shown by the natural species. In recent years, particle swarm optimization has appeared as a new and popular optimization algorithm due to its simplicity and efficiency. The role of the PSO in this study is to suggest an adequate adjustment of the parameters (kp, Ki, Kd) to satisfy some drive system requirements.

In last years, the FLC has improved results of nonlinear and complex processes [33]. The main idea of this approach is that it does not need a precise mathematical model of the electric machine, FLCs are robust and their performance is insensitive to parameter variations. With the increasing evolution of approximation theory, the adaptive control methods have been presented to cope with the nonlinear systems with parametric uncertainty based on fuzzy logic system (FLS) [34], neural networks (NNs) [35], adaptive fuzzy and NN control approaches via backstepping methods [36,37].

There are two disadvantages in the conception of a FLC. The first one is the obtaining of a suitable rule-base for the application, while the second is the selection of scaling factors prior to fuzzification and after defuzzification, in order to overwhelm these drawbacks and expedite the determination of the design parameters and to reduce the time consumption. Several solutions are adapted to remedy these problems. In [38,39] the authors presents an on line method for adapting the scaling factors of the FLC, the authors suggest a solution to design an adaptive fuzzy controller. The objective of the proposed form is to adapt online scaling factors according to a performance measure in order to refine the controller and increase the performance of the drive system.

In this paper, we investigate the performance of PSO for optimizing the gains of the fuzzy-PID speed controller of the DSIM.

2. Modeling of the dual star induction motor

The DSIM dynamic equations in the reference d-q can be reported as follow [4]:

$$\begin{cases} V_{ds1} = R_{s1} i_{ds1} + \dfrac{\mathrm{d}\,\psi_{ds1}}{\mathrm{d}t} - \omega_s \psi_{qs1} \\ V_{qs1} = R_{s1} i_{qs1} + \dfrac{\mathrm{d}\,\psi_{qs1}}{\mathrm{d}t} + \omega_s \psi_{ds1} \\ V_{ds2} = R_{s2} i_{ds2} + \dfrac{\mathrm{d}\,\psi_{ds2}}{\mathrm{d}t} - \omega_s \psi_{qs2} \\ V_{qs2} = R_{s2} i_{qs2} + \dfrac{\mathrm{d}\,\psi_{qs2}}{\mathrm{d}t} + \omega_s \psi_{ds2} \\ V_{dr} = 0 = R_r i_{dr} + \dfrac{\mathrm{d}\,\psi_{dr}}{\mathrm{d}t} - (\omega_s - \omega_r)\psi_{qr} \\ V_{qr} = 0 = R_r i_{qr} + \dfrac{\mathrm{d}\,\varphi_{qr}}{\mathrm{d}t} + (\omega_s - \omega_r)\varphi_{dr} \end{cases} \tag{1}$$

where the fluxes equations are:

$$\begin{cases} \psi_{ds1} = L_{s1} i_{ds1} + L_m(i_{ds1} + i_{ds2} + i_{dr}) \\ \psi_{qs1} = L_{s1} i_{qs1} + L_m(i_{qs1} + i_{qs2} + i_{qr}) \\ \psi_{ds2} = L_{s2} i_{ds2} + L_m(i_{ds1} + i_{ds2} + i_{dr}) \\ \psi_{qs1} = L_{s1} i_{qs1} + L_m(i_{qs1} + i_{qs2} + i_{qr}) \\ \psi_{dr} = L_r i_{dr} + L_m(i_{ds1} + i_{ds2} + i_{dr}) \\ \psi_{qr} = L_r i_{qr} + L_m(i_{qs1} + i_{qs2} + i_{qr}) \end{cases} \tag{2}$$

For studying the dynamic behavior, the following equation of motion was added:

$$J \frac{\mathrm{d}\Omega_r}{\mathrm{d}t} = \mathrm{T}_{em} - \mathrm{T}_r - f_r \Omega_r \tag{3}$$

The model of the DSIM has been completed by the expression of the electromagnetic torque T_{em} given below:

$$\mathrm{T}_{em} = p\frac{L_m}{L_m + L_r}\left(\psi_{dr}(i_{qs1} + i_{qs2}) - \psi_{qr}(i_{ds1} + i_{ds2})\right) \tag{4}$$

A schematic representation of the stator and rotor windings of dual star induction motor is given in Figure 1.

3. Direct torque control (DTC) of the DSIM

The classical DTC, proposed by [40], is based on the following algorithm:

- Divide the time domain into periods of reduced duration Ts;
- For each clock struck, measure the line currents and phase voltages of the DSIM;
- Reconstitute the components of the stator flux vector and estimate the electromagnetic torque, through the estimation of the stator flux vector and the measurement of the line current;
- The error between the estimated torque and the reference one is the input of a three level hysteresis comparator when this latter generates at its output the value of +*1* to increase the flux and *0* to reduce it and thus increasing the torque –*1* it reduce this flux and *0* to keep it constant in a band;
- The error between the estimated stator flux magnitudes is the input of a two levels of the hysteresis comparator, which generates at its output the value +*1* to increase the flux and *0* to reduce it;
- Select the state of the switches to determine the operating sequences of the inverter using the switching table. The input quantities are the stator flux sector and the outputs of the two hysteresis comparators.

The block diagram of the DTC of DSIM is shown in Figure 2.

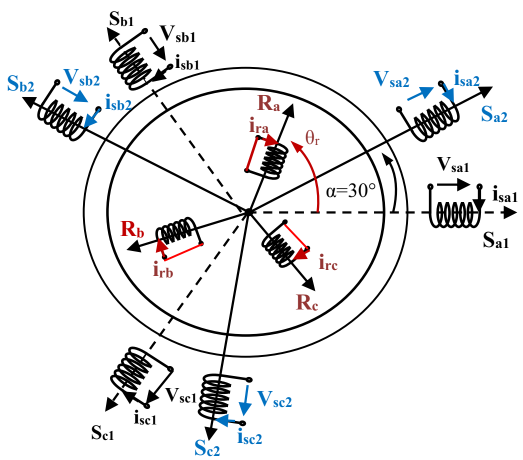

Figure 1.
Schematic representation of dual star induction motor (DSIM).

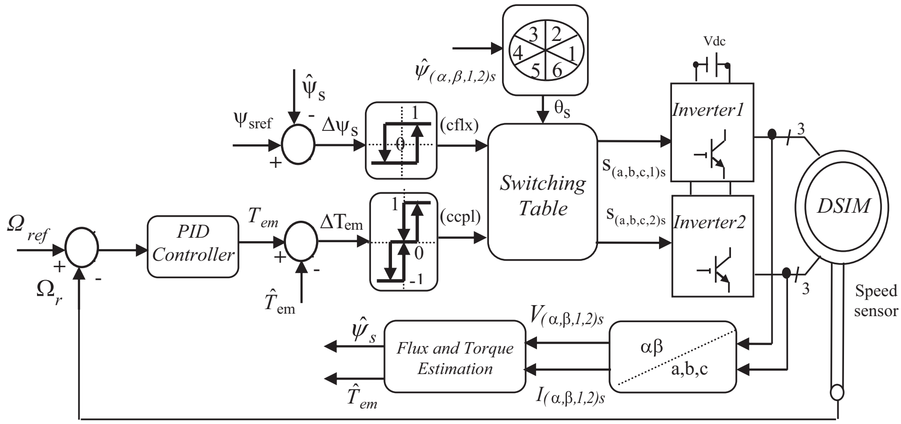

Figure 2.
Block diagram of the DTC of DSIM.

Moreover, Table 1 presents the sequences corresponding to the position of the stator flux vector to the different sectors. The flux and the torque are controlled by two hysteresis comparators at 2 and 3 levels, respectively, in the case of a two-level voltage inverter Table 5.

The expression of the stator flux is described by:

$$\begin{aligned} \psi_{s\alpha1.2} &= \int_0^t (V_{s\alpha1,2} - R_s i_{s\alpha1,2})dt \\ \psi_{s\beta1.2} &= \int_0^t (V_{s\beta1,2} - R_s i_{s\beta1,2})dt \end{aligned} \tag{5}$$

where $V_{s\alpha1,2}$ and $V_{s\beta1,2}$ are the estimated components of the stator vector voltage. They are expressed from the model of the inverter.

4. Particle swarm optimization algorithm

PSO uses a population of individuals to discovery the high solution in a search area among the neighboring solutions. The individual is defined by a particle, which displaces stochastically in the guidance of its preceding finest position and the best past location of the swarm.

Presume that the size of the swarm is n and the search area is m , next the position of the ith particle is given as xi=(x_{i1}, x_{i2},. . ... . . ,x_{id}). The finest previous positions of the ith particle are considering by [32]:

cflx	ccpl	1	2	3	4	5	6	Corrector
0	1	V_2	V_3	V_4	V_5	V_6	V_1	2 levels
	0	V_7	V_0	V_7	V_0	V_7	V_0	
	−1	V_6	V_1	V_2	V_3	V_4	V_5	3 levels
1	1	V_3	V_4	V_5	V_6	V_1	V_2	2 levels
	0	V_0	V_7	V_0	V_7	V_0	V_7	
	−1	V_5	V_6	V_1	V_2	V_3	V_4	3 levels

Table 1.
Control strategy with hysteresis comparator.

$$pbest_i = (pbest_{i1}, pbest_{i2}, \ldots, pbest_{id}) \tag{6}$$

The index of the best particle amongst the group is $gbest_d$. The velocity of particle *ith* is represented as:

$$v_i = (v_{i1}, v_{i2}, \ldots., v_{id}) \tag{7}$$

The modified speed and position of each particle can be calculated using the current and the distance from $pbest_{i,d}$ to $gbest_d$ as expressed in the following equations:

$$v^{t+1}_{i.m} = \underbrace{w.v^{t}_{i.m}}_{\text{inertia}} + \underbrace{C_1 * rand() * \left(pbest_{i,m} - X^{t}_{i,m}\right)}_{\text{personelinfluence}} + \underbrace{C_2 * rand() * \left(gbest_{i,m} - x^{t}_{i,m}\right)}_{\text{socialinfluence}} \tag{8}$$

$$x^{t+1}_{i,m} = x^{t}_{i,m} + v^{t+1}_{i,m} \quad i = 1, 2, \ldots, n; \quad m = 1, 2, \ldots, d \tag{9}$$

where: n is the number of particles in the group, d is the dimension index, t is the pointer of iterations (generations), $v^{t}_{i,m}$ is the velocity of particle at iteration i, w is the inertia weight factor, *rand ()* is the random number between *0* and *1*, $pbest_i$ is the best previous position of the *ith* particle, *gbest* is the best particle among all the particles in the population, C_1, C_2 are acceleration constant. Velocity vector for position update is depicted in Figure 3.

4.1 Algorithm steps for PSO

The working of PSO algorithm is interpreted in the consecutive steps.

Step 1: We establish the values of PSO algorithm constants as an inertia weight factor W = 0.8, with acceleration constants C1 = C2 = 2. The PSO main program has to optimize in this case three parameters, K_e, K_d and β to the fuzzy controller, and search optimal value of the three-dimensional search space.

Step 2: So we arbitrarily configured a swarm of "50" population in three-dimensional search space using (x_{i1}, x_{i2}, x_{i3}), and (v_{i1}, v_{i2}, v_{i3}) as preliminary situation along with velocity. Considered the primary fitness function of any also to the position with minimum fitness function is displayed as best, so the optimal fitness function as pbest1.

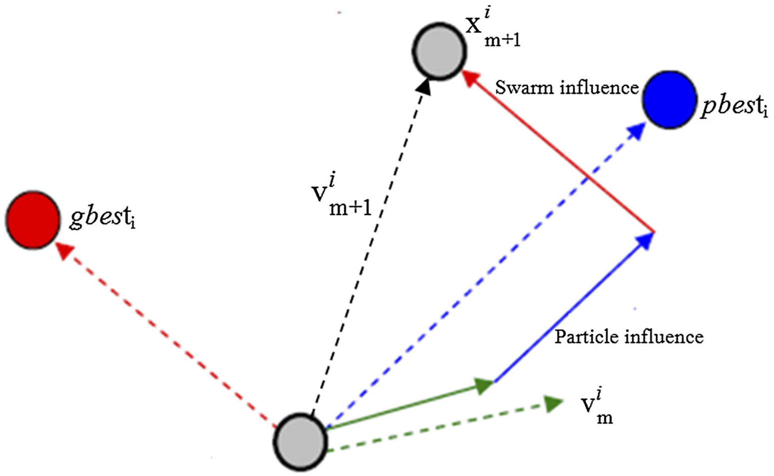

Figure 3.
Description of a searching point by PSO.

Step 3: Run the program by means of PSO algorithm through n numbers of iterations, as well, the program finds the final optimal value of the fitness function as "best fitness" with the last overall optimal point as "gbest". The PSO parameters are described in Table 2 in the Appendix.

The flowchart for fuzzy PSO-DTC-DSIM is shown in Figure 4.

4.2 Fitness function

4.2.1 The conception of fitness function. To evaluate the static and dynamic conduct of the control system, it is found that IAE offers good system stability with reduced oscillations the IAE criterion is widely adopted [41]:

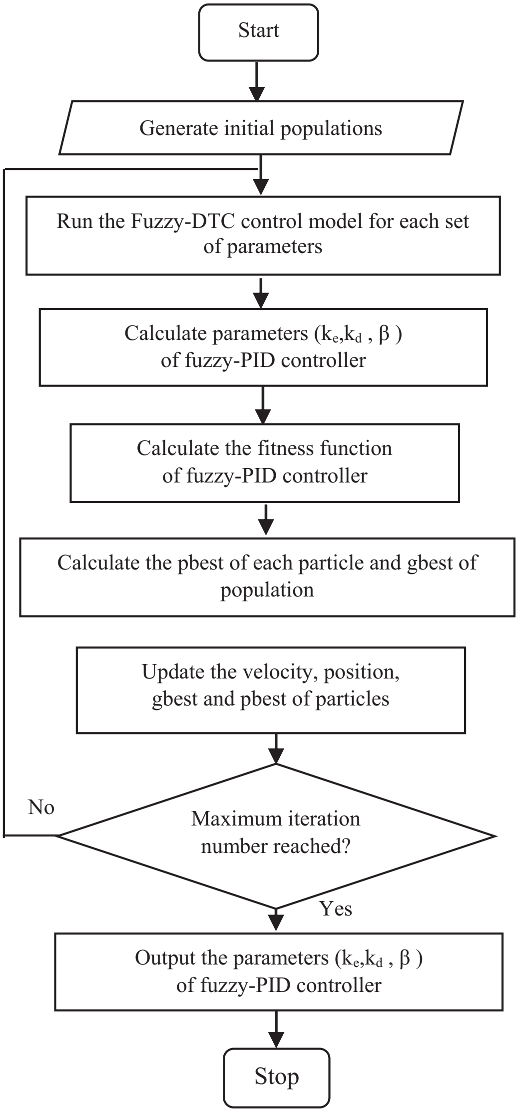

Figure 4.
Flowchart for fuzzy PSO-DTC-DSIM.

$$IAE = \int_{0}^{\infty} |e(t)|dt \tag{10}$$

5. Design of PID-PSO controller type FLC for the DSIM

The optimization of the FLC gains using PSO can be given by the input variable {e}, and the error change {e_c} as follows:

$$e(t) = \Omega_{ref} - \Omega_r(t) \tag{11}$$

$$e_c(t) = \frac{de(t)}{dt} \tag{12}$$

Table 3 illustrated the performance of PID controller in the Appendix

The fuzzy PI controller is the commonly used because the PD one encounters difficulties in deleting the steady state error. However, the fuzzy-PI gives a poor performance in the transient response in higher order systems because of its inherent internal integration operation. It is therefore more convenient to combine PI and PD actions to design a fuzzy PID controller (FLC-PID) to achieve proportional, integral, and derivative control action. It is imperative to obtain an FLC-PID controlled by adding the fuzzy-PD controller output and its embedded part. The fuzzy-PID controller is depicted in Figure 5. Table 4 represented the performance of fuzzy controller is in the Appendix.

Descriptions	Parameters
Number of particles in the swarm	50
Number of Iterations	10
Number of components or dimension	3
Inertia weight factor w	0.8
C1=C2	2

Table 2.
Parameters of PSO algorithms.

Controllers	Parameters
K_p	37.5
K_i	0.35
K_d	0

Table 3.
Performance of PID controller.

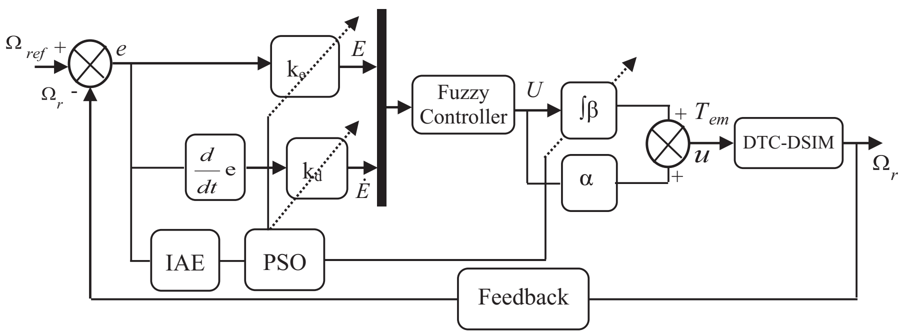

Figure 5.
The proposed control structure for PID-PSO type FLC.

The output u of the fuzzy PID is presented by:

$$u = \alpha U + \int \beta U \ dt \tag{13}$$

where: U is the output of the FLC.

The relationship between the input and output variables is given by [42]:

$$U = A + PE + D \ dE/dt \tag{14}$$

where: $E = K_e.e$ and dE/dt = $Kd.de/dt$ according to Figure 5.

Therefore, from Eqs. (13) and (14) the controller output is expressed by the following equation:

$$u = \alpha A + \beta A.t + \alpha K_e.Pe + \beta K_d.D.e + \beta K_e.P \int edt + \alpha K_d.D.de/dt \tag{15}$$

Finally, the components of PID-FLC can be deducted as follows:

The proportional gain: $\alpha K_e.\ P{+}\beta K_d.D;$ The integral gain: $\beta\ K_e.P;$ The derivative gain: $\alpha K_d.D.$

5.1 Fuzzification

The inputs to the Fuzzy-PSO have to be fuzzified before being fed into the control rule and gain rule determinations. The triangular membership functions (*MFs*) used for the input (e, e_c and, ΔT_{em}) are shown in Figures 6 and 7. Linguistic variables are (NB, NM, NS, ZE, PS, PM, PB).

Where: NB is Negative Big, NM is Negative Medium, NS is Negative Small, EZ is Equal Zero, PS is Positive Small, PM is Positive Medium, PB is Positive Big.

5.2 Inference and defuzzification

The present paper uses MIN operation for the calculation of the degree $\mu(\Delta T_{em})$ associated with every rule, for example, $\mu(\Delta T_{em}) = Min[\mu(e),\mu(e_c)]$.

In the defuzzification stage, a crisp value of the electromagnetic torque is obtained by the normalized output function as [33]:

$$du = \frac{\sum_{j=1}^{m} \mu(\Delta T_{emj})\Delta T_{emj}}{\sum_{j=1}^{m} \mu(\Delta T_{emj})} \tag{16}$$

where: m is the total number of rules *(7*7)*, $\mu(\Delta T_{em})$ is the membership grade for the n rule, ΔT_{em} is the position of membership functions in rule n in U (−15,−10,-5,0,10,15).

Table 4.
Performance of fuzzy-PSO controller.

Controller	Fuzzy-PSO
Input scaling factor k_e optimized	3.1604
Input scaling factor k_d optimized	3.6741
β is the gain of the integral component	0.8081
α scaling factor for the output u	1

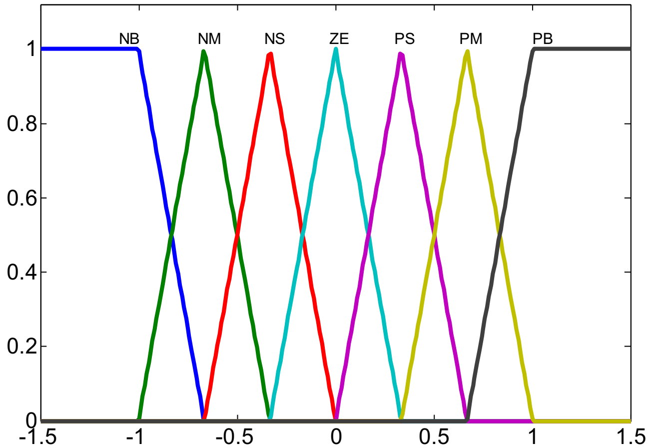

Figure 6.
Membership functions for e and e_c.

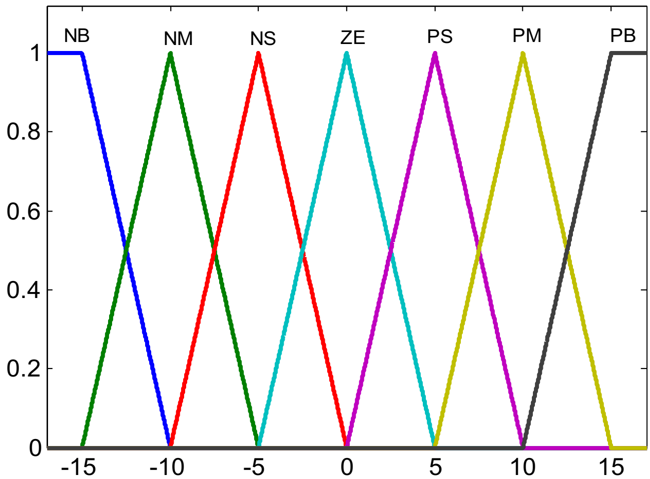

Figure 7.
Membership functions for ΔT_{em}.

5.3 Control rule determination

The logic of determining this rule matrix is based on a global knowledge of the system operation. As an example, we consider the following two rules:

if *e* is PB and *ec* is PB then ΔTem is PB

if *e* is ZE and *ec* is ZE then ΔTem is ZE

They indicate that if the speed is too small compared to its reference (*e* is *PB*), so a big gain (ΔT_{em} is *PB*) is required to bring the speed to its reference and if the speed reaches its reference and is established (*e* is *ZE* and e_c is *ZE*) so impose a small gain ΔT_{em} is ZE.

Table 5 represents the inference rules.

6. Simulation results and discussion

The results were obtained using a PSO algorithm programmed and implemented in MATLAB. The parameters of the DSIM are presented in Table 6 (Appendix). To illustrate the performances of the DTC of the DSIM we replaced the classical PID controller by a fuzzy-PSO technique in Figure 8. The simulation is carried out under the following conditions: the hysteresis band of the torque comparator is set to ± 0.25 Nm and that of the flux comparator to $\pm$ *0.5 Wb*.

Figure 9 depicts the waveforms of the improved performances of speed control. It can be noticed that the use of the fuzzy-PSO controller allows the speed to judiciously follow its reference value of *100 rad/s* despite the presence of a load torque of *14Nm* at $t = 0.6$ *s*. In fact, this behaviour represents a clear improvement in dynamic response with a hybrid controller

Table 5.
Inference rules.

ΔT_{em}		e_c						
		NB	NM	NS	ZE	PS	PM	PB
E	NB	NB	NB	NB	NB	NM	NS	ZE
	NM	NB	NB	NB	NM	NS	ZE	PS
	NS	NB	NB	NM	NS	ZE	PS	PM
	ZE	NB	NM	NS	ZE	PS	PM	PB
	PS	NM	NS	ZE	PS	PM	PB	PB
	PM	NS	ZE	PS	PM	PB	PB	PB
	PB	ZE	PS	PM	PB	PB	PB	PB

Table 6.
DSIM parameters [12].

Rated Power	4.5KW
Stator Resistance $R_{s1} = R_{s2}$	3.72Ω
Rotor Resistance R_r	2.12Ω
Stator Inductance L_s	0.022H
Rotor Inductance L_r	0.006H
Mutual Inductance L_m	0.3672H
Pole Pairs P	1
Machine Inertia J	0.0662 kg.m2
Viscous Friction Coefficient f_r	0.001 kg.m2/s

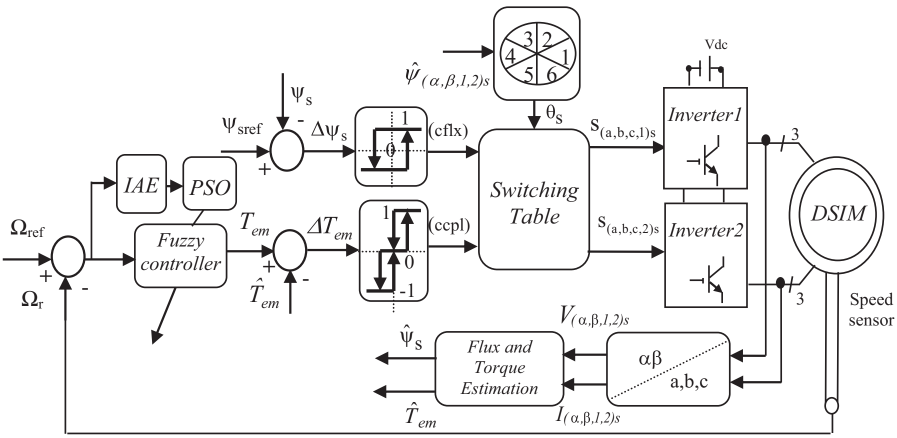

Figure 8.
Block diagram of the proposed DTC-fuzzy-PSO tuning speed controller.

that is adjusting strictly the values of the parameters by increasing the constant of integration without an overshoot at the level of the dynamic response of the speed, contrary to a drive with a standard DTC-PID where the speed has underwent slightly rejected.

Performance with each controller is also analyzed through these of Integral Squared Error (ISE), Integral Absolute Error (IAE) and Integral Time Squared Error (ITSE), and the results described in Table 7 confirm the improved performance with the fuzzy-PSO algorithm.

In Figure 10 the electromagnetic torque produced by the DSIM controlled by DTC-PID and DTC-fuzzy-PSO is presented. In this figure, it can be noticed that the ripple is not the same for the two techniques. It is clear that the classical DTC-PID present two problems, steady state error and high torque ripples. On the other hand, the DTC-fuzzy-PSO corrects the steady state error and reduces the torque ripples.

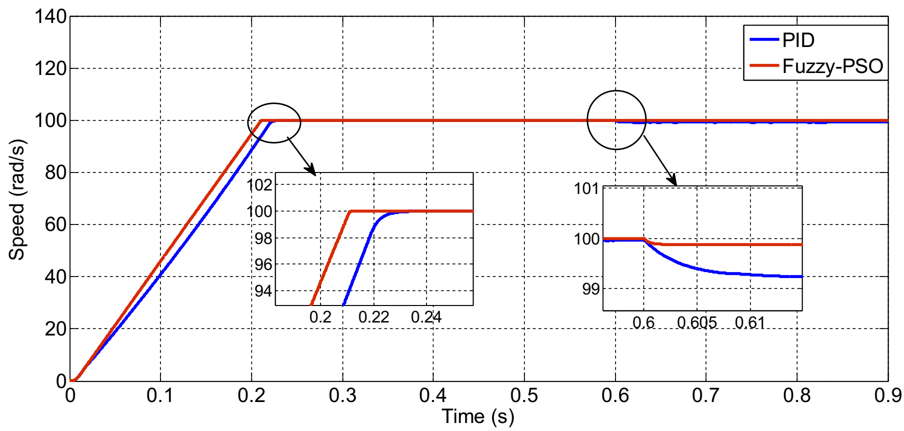

Figure 9. Comparison of the rotor speed regulation of the standard DTC and hybrid DTC.

Controllers	IAE	ISE	ITSE
PID	0.5473	0.1498	0.1348
Fuzzy-PSO	0.2072	0.0215	0.0193

Table 7. Comparison of performance index.

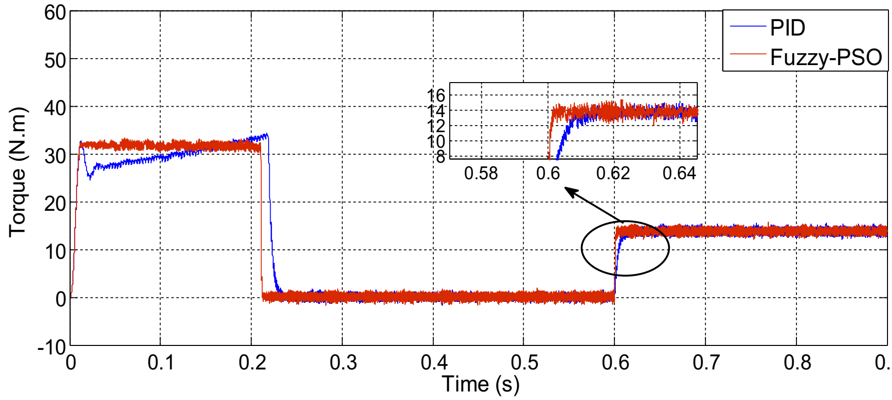

Figure 10. Electromagnetic torque comparison of the two strategies.

In Figure 11, it can be observed that the currents are sinusoidal and current ripples have also a notable reduction in fuzzy-PSO controller compared to the standard controller.

Figure 12 shows the trajectory of stator flux for the standard DTC and the hybrid DTC. It can be seen that this hybrid strategy has less ripple.

Figure 13 summarizes the evolution of the fitness function with respect to the number of iterations.

7. Conclusion

In this paper, a comparative study between the conventional DTC of the DSIM with PID controller and DTC-fuzzy-PSO has been presented for a speed controller. From the simulation studies, hybrid controller produced better performances in terms of a fast rise time, a small overshoot, reduced torque and flux ripples. Therefore very satisfactory performances have been achieved. Furthermore, the effectiveness of the proposed algorithms is evaluated and justified from performance indices IAE, ISE and ITSE. According to the yielded simulation results one can conclude that this algorithm is suitable for applications requiring a high

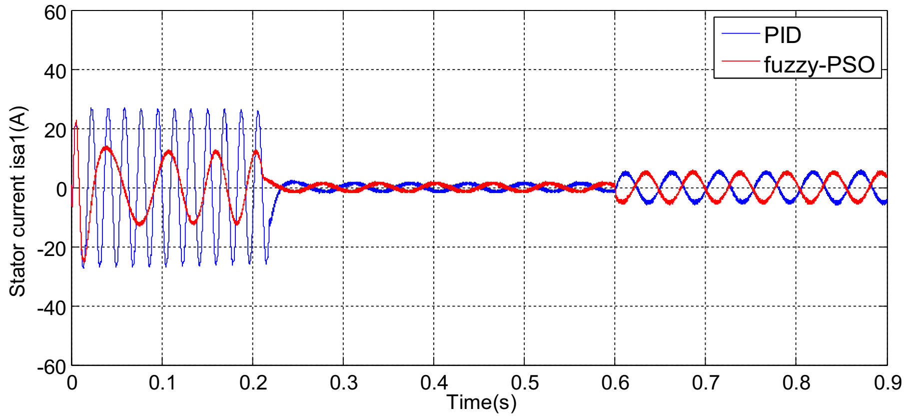

Figure 11.
Phase current in the stator 1for both hybrid DTC and standad DTC.

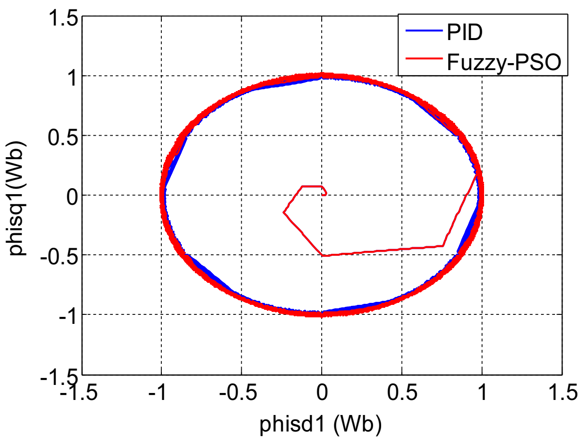

Figure 12.
Stator flux trajectory in the stator1.

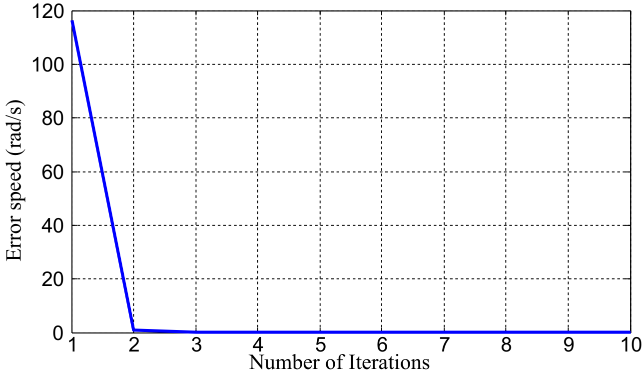

Figure 13.
Evolution of the fitness function relative to Fuzzy-PSO algorithm.

tracking accuracy in presence of external disturbances. In future, the work can be extended by the applications of the intelligent hybrid techniques like neuro-fuzzy-GA, neuro-fuzzy-PSO, neuro-fuzzy-ACO.

Abbreviations

DSIM	dual star induction motor
FLC	fuzzy logic controller
PSO	particle swarm optimization
DTC	direct torque control
PID	proportional integral derevative
IAE	the integral of absolute value of the error
ISE	the integral of square error
ITSE	the integral of time multiply square error

References

[1] Y. Zhao, T.A. Lipo, Space vector PWM control of dual three-phase induction machine using vector space decomposition, IEEE Trans. Ind. Appl. 31 (5) (1995) 1100–1108.

[2] D. Hadiouche, H. Razik, A. Rezgzou, On the modeling and design of dual-stator windings to minimize circulating harmonic currents for VSI fed AC machines, IEEE Trans. Indus. Appl. 40 (2) (2004) 506–515.

[3] G.K. Singh, Multi-phase induction machine drive research-a survey, Electr. Power Sys. Res. 61 (2) (2002) 139–147.

[4] H.S. Che, E. Levi, M. Jones, M.J. Duran, W.P. Hew, N.A. Rahim, Operation of six-phase induction machine using series-connected machine-side converters, IEEE Trans. Ind. Electron. 61 (2015) 164–176.

[5] S. Basak, C. Chakraborty, Dual stator winding induction machine, Problems, , Progress, and Future Scope IEEE Trans. Ind. Electron. 62 (7) (2015) 4641–4652.

[6] K. Pieńkowski, Analysis and control of dual stator winding induction motor, Arch. Electric. Eng. 61 (3) (2012) 421–438.

[7] I. Kortas, A. Sakly, M.F. Mimouni, Optimal vector control to a double-star induction motor, Energy 13 (4) (2017) 279–288.

[8] B. Tabbache, S. Douida, M. Benbouzid, D. Diallo, A. Kheloui, Direct torque control of five-leg inverter-dual induction motor powertrain for electric vehicles, Electric. Eng. 99 (3) (2017) 1073–1085.

[9] M. Bouziane, M. Abdelkader, A neural network based speed control of a dual star induction motor, Int. J. Electric. Comput. Eng. 4 (6) (2014) 952–961.

[10] H. Mesloub, M.T. Benchouia, A. Goléa, N. Goléa, M.E.H. Benbouzid, A comparative experimental study of direct torque control based on adaptive fuzzy logic controller and particle swarm optimization algorithms of a permanent magnet synchronous motor, Int. J. Adv. Manuf. Technol. (2016).

[11] D. Azib, T. Ziane, A. Rekioua, S. Tounzi, Robustness of the direct torque control of double star induction motor in fault condition, Rev. Roum. Sci. Techn. Électrotechn. et Énergn 61 (2) (2016) 147–152.

[12] A. Taheri, Harmonic reduction of direct torque control of six-phase induction motor, ISA Trans. 63 (2) (2016) 299–314.

[13] S. Meroufel, A. Massoum, A. Bentaallah, P. Wira, Double star induction motor direct torque control with fuzzy sliding mode speed controller, Rev. Roum. Sci. Techn. Electrotechn. et Energ. 62 (4) (2017) 31–35.

[14] B. Larafi, R. Abdessemed, K. Abdelhalim, E. Merabet, Control neuro-fuzzy of a dual star induction machine (DSIM) supplied by five-level inverter, J. Power Technol. 98 (1) (2018) 70–79.

[15] P. Vega, C. Prada, V. Aleixander, Self-tuning predictive PID controller, IEE Proc. 138 (3) (1991) 303–311.

[16] E. Merabet, H. Amimeur, F. Hamoudi, R. Abdessemed, Self tuning fuzzy logic controller for a dual star induction machine, J. Electric. Eng. Technol. 6 (4) (2011) 33–54.

[17] N. Farah, M.H.N. Talib, Z. Ibrahim, M. Azri, Z. Rasin, "Self-tuned output scaling factor of fuzzy logic speed control of induction motor drive", in: 7th IEEE International Conference on System Engineering and Technology, 2–3 October Malaysia, (2017).

[18] E.S. Ali, Speed control of induction motor supplied by wind turbine via imperialist competitive algorithm, Energy 89 (2015) 593–600.

[19] D. Wu, Z. Huimin, Z. LI, L. Guangyu, Y. Xinhua, W. Daqing, A novel collaborative optimization algorithm in solving complex optimization problems, Soft comput. 21 (15) (2017) 4387–4398.

[20] D. Sivamani, R. Harikrishnan, R. Essakiraj, Genetic algorithm based PI controller for DC-DC converter applied to renewable energy applications, Int. J. Pure Appl. Mathemat. 118 (16) (2018) 1053–1071.

[21] S. Zemmit, A. Messalti, A. Harrag, A new improved DTC of doubly fed induction machine using GA-based PI controller, Ain Shams Eng. J. 8 (4) (2017) 481–706.

[22] E.S. Ali, Optimization of power system stabilizers using BAT search algorithm, Int J Electr Power Energy Syst. 61 (no. C) (2014) 683–690.

[23] Y. Bekakra, D. Ben, Attous, "Optimizing of IP speed controller using particle swarm optimization for FOC of an induction motor", Int. J. Syst. Assur. Eng. Manage. (2015).

[24] P. Nammalvar, S. Ramkumar, Parameter improved particle swarm optimization based direct-current vector control strategy for solar PV system, Adv. Electric. Comput. Eng. 18 (1) (2018) 3628–3648.

[25] K. Dezelak, P. Bracinik, M. Hoger, A. Otcenasova, Comparison between the particle swarm optimisation and differential evolution approaches for the optimal proportional–integral controllers design during photovoltaic power plants modelling, IET Renew. Power Generat. 10 (4) (2016) 522–530.

[26] O.P. Bharti, R.K. Saket, S.K. Nagar, Controller design for doubly fed induction generator using particle swarm optimization technique, Renewable Energy 114 (1) (2017) 1394–1406.

[27] A.S. Oshaba, E.S. Ali, S.M. Abd Elazim, ACO based speed control of SRM fed by photovoltaic system, Int. J. Electric. Power Energy Syst. 67 (2015) 529–536.

[28] L.C. Bruno, L.G. Clayton, A.A. Bruno, G. Alessandro, F.C. Marcelo, Metaheuristic optimization applied to PI controllers tuning of a DTC-SVM drive for three-phase induction motors, Appl. Soft Comput. 62 (2018).

[29] H. Garg, A hybrid PSO-GA algorithm for constrained optimization problems, Appl. Mathemat. Comput. 274 (2) (2016) 1292–1305.

[30] A. Gacem, D. Benattous, Hybrid GA–PSO for optimal placement of static VAR compensators in power system, Int. J. Syst. Assur. Eng. Manage. (2015).

[31] M. Mareli, B. Twala, An adaptive Cuckoo search algorithm for optimisation, Appl. Comput. Informat. 14 (2) (2018) 107–115.

[32] R. Eberhart, J. Kennedy, A new optimizer using particles warm theory", Proceedings of the Sixth International Symposium on Micro Machine and Human Science, Japan (1995) 39–43.

[33] Z. Tir, O.P. Malik, A.M. Eltamaly, Fuzzy logic based speed control of indirect field oriented controlled double star induction motors" connected in parallel to a single six-phase inverter, Electric Power Syst. Res. 134 (1) (2016) 126–133.

[34] J.P. Yu, P. Shi, W. Dong, C. Lin, Command filtering-based fuzzy control for nonlinear systems with saturation input, IEEE Trans. Cybernet. 47 (9) (2017).

[35] J.P. Yu, B. Chen, H. Yu, C. Lin, L. Zhao, Neural networks-based command filtering control of nonlinear systems with uncertain disturbance, Informat. Sci. 426 (2018) 50–60.

[36] J.P. Yu, P. Shi, W. Dong, C. Lin, Adaptive fuzzy control of nonlinear systems with unknown dead zones based on command filtering, IEEE Trans. Fuzzy Syst. 26 (1) (2018).

[37] Z. Zhou, J.P. Yu, H. Yu, C. Lin, Neural network-based discrete-time command filtered adaptive position tracking control for induction motors via backstepping, Neurocomputing 260 (2017) 203–210.

[38] J. Huang, J. Wang, H. Fang, An anti-windup self-tuning fuzzy PID controller for speed control of brushless DC motor, , Automatika, J. Control Measure. 58 (3) (2018) 321–335.

[39] O. Karasakal, E. Yesil, M. Guzelkaya, I. Eksin, Implementation of a new self-tuning fuzzy PID controller on PLC, Turk. J. Elec. Eng. 13 (2) (2005).

[40] I. Takahashi, T. Noguchi, A new quick-response and high-efficiency control strategy of an induction motor, IEEE Trans. Indust. Appl. 22 (5) (1986) 820–827.

[41] S. Kavita, C. Varsha, S. Harish, C.B. Jagdish, Fitness based particle swarm optimization, Int. J. Syst. Assur. Eng. Manage. 6 (3) (2015) 319–329.

[42] W.Z. Qiao, M. Mizumoto, PID type fuzzy controller and parameters adaptive method, Fuzzy Sets Syst. 78 (2) (1996) 23–35.

Appendix

See.

Corresponding author

Sebti Belkacem can be contacted at: belkacem_sebti@yahoo.fr